Available online at www.sciencedirect.com
SCIENCE DIRECT®
Sensors and Actuators A 121 (2005) 162–171
SENSORS AND ACTUATORS A PHYSICAL
www.elsevier.com/locate/sna

A slim type microvalve driven by PZT films

Hyonse Kim[a], Chihyun In[b], Gilho Yoon[a], Jongwon Kim[a,*]

[a] *School of Mechanical and Aerospace Engineering, Seoul National University, Shinlim-Dong, San 56-1, Kwanak-Gu, Seoul 151 742, Republic of Korea*
[b] *MEMS Division, DAEWOO Electronics Corp., Kasan-dong, Kumchun-gu, Seoul 153 801, Republic of Korea*

Received 28 May 2004; received in revised form 30 November 2004; accepted 6 December 2004
Available online 18 January 2005

Abstract

A slim type microvalve actuated by PZT films was developed. Three different sizes of microvalves having a thickness of 528 μm were designed. Each one has 120 cantilevers arrayed circularly. In designing them, tip deflections of PZT cantilevers were calculated, and compared with those obtained by FEM simulations. Leakage and flow rate were calculated. Fabrication process and the PZT film deposition process are explained. The microvalve structure with PZT films was fabricated on a SiO_2 layer over a supporting silicon on insulator (SOI) wafer. The ferroelectric properties of PZT films were studied with polarization–voltage (*P–V*) and dielectric constant, dielectric loss-voltage measurement. Tip deflections were measured on the fabricated array, applied with different voltages. Tip displacement of 12 μm (Φ = 10 mm-type) was obtained with the applied voltage of 5 V. When the microvalve was closed, the air leakage was 15 μl/s. The air-flow rate of 122 μl/s (Φ = 10 mm-type) was measured with the pressure difference of 1000 Pa in the opened position at 15 V.

Keywords: Microvalve; Micro cantilever; PZT film; Micro fluidic system

1. Introduction

The microvalve is a crucial part of a microfluidic system. Passive and active microvalves have been actively researched. Passive microvalves are checked valves or flap valves that regulate fluid flow in one direction without actuation. Thus, they can be applied only to micropumps. In contrast, active microvalves can be controlled with actuation, so they are considered more important in micro fluidic systems.

Active microvalves have been controlled by various actuating methods such as thermopneumatic [1], piezoelectric [2], electromagnetic [3], bimetallic [4], and shape memory [5] methods. Selvaganapathy et al. [1] presented an electrothermally actuated inline microvalve, for which actuators use the high volumetric expansion of a sealed patch of paraffin heated above its melting point, to provide displacements and forces while using power. Roberts et al. [2] reported a compact piezoelectrically driven hydraulic amplification microvalve. But piezoelectric actuators require high operating voltage. Capanu et al. [3] presented a bistable electromagnetically actuated microvalve. Bistability was achieved by balancing the elastic force of a cantilever with the magnetic forces of a permanent magnetic foil and electromagnetic coil. Jerman [4] used an aluminum layer on a Si membrane for actuating a normally closed thermal bimorph. But the thermal bimorph can actuate under high temperature. Pemble and Towe [5] used a shape memory alloy for actuation. This actuation method can work at relatively low temperature and low voltage, but the Martensitic transformation temperatures are sensitive to the trace alloy elements and the thin-film processing is difficult [3].

Recently, piezoelectric PZT films have been widely used for sensors and actuators in micro-electromechanical systems (MEMS) because they offer high ferroelectric and piezoelectric characteristics [6,7,8]. Actuation applications were given by Koch et al. [9] who proposed a micromachined pump based on thick-film piezoelectric actuation, and by Flynn

* Corresponding author. Tel.: +82 2 880 7138; fax: +82 2 875 4848.
E-mail address: jongkim@snu.ac.kr (J. Kim).

0924-4247/$ – see front matter © 2004 Elsevier B.V. All rights reserved.
doi:10.1016/j.sna.2004.12.005

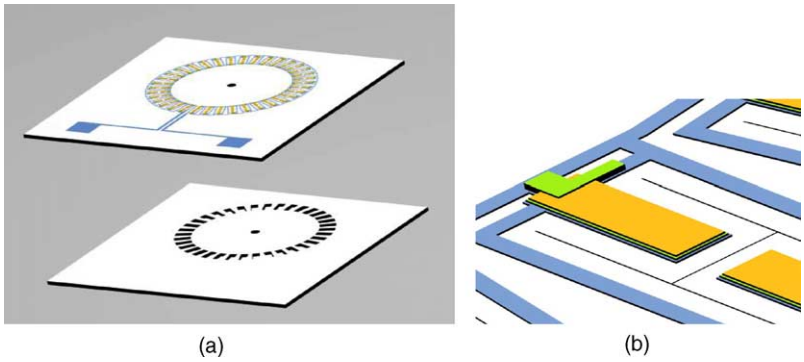

Fig. 1. (a) Schematics of the microvalve and (b) magnified view of a sub-unit.

et al. [10] who reported piezoelectric micromotors for microrobots. Kueppers et al. [11] presented the integration of sol–gel PZT thin-films on silicon cantilever structures for micromirror and microrelay applications. Gross et al. [12] reported a piezoelectric micro-electromechanical switch actuated by a PZT cantilever. However, no previous work has been done on microvalves driven by PZT films.

We present an ultra slim microvalve of different sizes, which are actuated by PZT films. We defined a slim type microvalve as a microvalve, which has a thickness that does not exceed 1000 μm except for a power supplier. The design features of the proposed microvalve are explained with the operating principle, piezoelectric design, and fluidic analysis. Its detailed fabrication process at each step is described, and the fabrication results are shown by SEM pictures. The tip deflections were measured, and were compared with analytical values and FEM analysis results. The performance of the microvalve was measured experimentally. The measured flow rate of air was compared with analytic solutions.

2. Microvalve design

The microvalve driven by PZT films was composed of multiple cantilevers that will move simultaneously. The design of PZT cantilevers was different from that of conventional micro cantilevers in previous applications such as atomic force microscopes (AFM). In AFM, quick response and high resonance frequency are preferable, so the size of cantilevers is small. In contrast, longer PZT cantilevers are preferred for actuator applications, which require a high tip deflection [11]. Furthermore, the cantilever shape was made differently from the pentagonal shape of general cantilevers to minimize fluid leakage. For micro fluidic systems, the microvalve require the following: (1) fluidic leakage of less than 20 μl/s in the closed position; (2) operating voltages from 1 to 15 V; (3) cantilever tip deflection of more than 45 μm in the opened position at 15 V; (4) ability to work with a maximum flow rate of 130 μl/s at 1000 Pa pressure difference; (5) opening and closing times of less than 1 s; and (6) device thickness of less than 600 μm.

2.1. Design features

We designed the microvalve by distributing 60 pairs of PZT cantilevers arrayed circularly and having three different sizes ($\Phi = 10$, 15, 20 mm). PZT cantilevers have right square shape and minimum gaps between it and the supporting structure to prevent leakage through the cantilevers. This design is illustrated in Fig. 1(a) and (b). The fabricated microvalve is shown in Fig. 2(a–c). Each type has 120 cantilevers in total, which will vibrate in synchronization. To reduce the leakage of the working fluid through the gap, we released the cantilevers at 4 μm intervals. We also enlarged the size of the cantilevers to a length of 450 μm and width of 300 μm, which is larger than general micro cantilevers that have been applied to micro sensors. Through this design, we were able to achieve more tip deflection and better fluid control. The connecting bridges from the top electrodes to the bottom electrodes have angled shapes that can contact to the bottom electrodes at two points. This design gives better chance of success in the lift-off fabrication process, which will be explained later in this paper. This design is illustrated in Fig. 1(b).

The working principle of the microvalve is illustrated in Fig. 3(a) and (b). When no voltage is applied to the microvalve, it will be in a closed position; when electric voltage is applied, it will be in an opened position to allow flow induced by the pressure difference between the inlet pressure P_1 and outlet pressure P_2.

2.2. Cantilever design

We estimated the displacement of the cantilever tip using Eq. (1). Tip deflection δ of the unimorph cantilever can be calculated as,

$$\delta = \frac{-3d_{31}s_{11}^{s}s_{11}^{p}h^{s}(h^{s}+h^{p})L^{2}}{K}V$$

$$K = (s_{11}^{s})^{2}(h^{p})^{4} + 4s_{11}^{s}s_{11}^{p}h^{s}(h^{p})^{3} + 6s_{11}^{s}s_{11}^{p}(h^{s})^{2}(h^{p})^{2} + 4s_{11}^{s}s_{11}^{p}h^{p}(h^{s})^{3} + (s_{11}^{s})^{2}(h^{s})^{4} \quad (1)$$

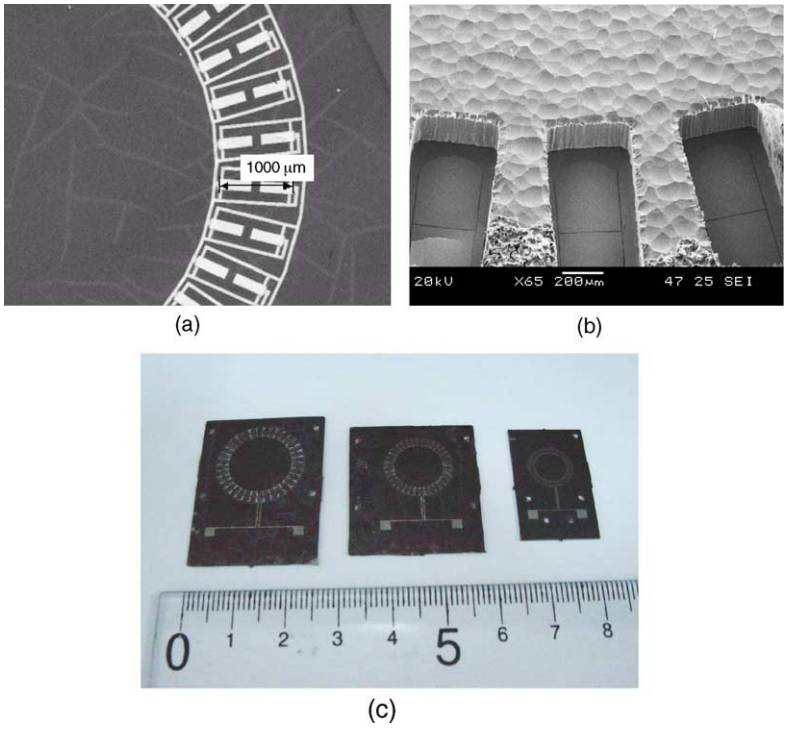

Fig. 2. The fabricated microvalves are shown by:(a) a front view SEM picture; (b) a backside view SEM picture; and (c) an overall picture of $\Phi = 20$, 15, and 10 mm-types from the left.

where V, d_{31}, h, s_{11}, L, K are the voltage applied between the top and bottom electrodes, the transverse piezoelectric coefficient, the thickness, the elastic compliance, the length of the cantilever and constant, respectively [13]. The superscripts of 's' and 'p' denote the substrate and the piezoelectric film, respectively. The influence of s_{21} was ignored because the elastic compliance in the x direction by the stress in the y direction is small and the width of the cantilever is smaller than the length. And the d_{33}, the longitudinal piezoelectric property, was also ignored because we assumed the no change in the thickness of the piezoelectric film since any amount of change was much smaller than that of the length of the cantilevers.

The transverse piezoelectric coefficient was obtained using Eq. (2).

$$d_{31} = e_{31} s_{11}^{\mathrm{p}} \tag{2}$$

where e_{31} is the piezoelectric coefficient. The elastic compliance s_{11} is given by the reciprocal of the Young's modulus. The Young's modulus of PZT is reported as 132 GPa [14] and that of Si is reported as 190 GPa [15]. The piezoelectric coefficient of the PZT films on a Si substrate was reported as -4.1 to $-6.0\,\mathrm{C/m^2}$ as applied voltages increase from 1 to 15 V [16]. The calculated deflections of each size of $\Phi = 10$, 15, and 20 mm were 14.8, 22.2, and 29.5 μm, respectively, at 5 V applied. The material properties of the micro cantilever are listed in Table 1. Tip deflections of the micro cantilever as a function of the applied voltage are shown in Fig. 4.

The behavior of the micro cantilever was predicted by structural simulation with ANSYS. The dimensions that were

Table 1
Material properties of the micro cantilever

Material	Young's modulus ($\mathrm{N/m^2}$)	Piezoelectric coefficient
PZT	1.32×10^{11}	-4.1 to $-6.0\,\mathrm{C/m^2}$ (applied voltage 1–15 V)
Si	1.90×10^{11}	

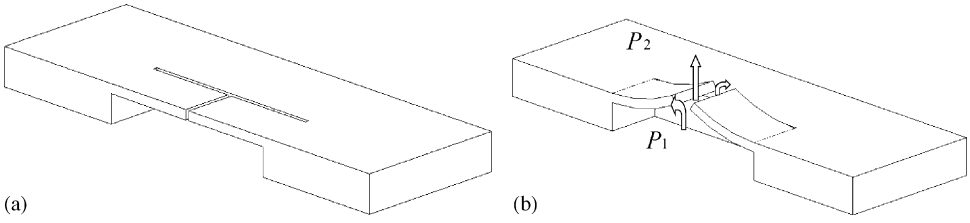

Fig. 3. Schematics of a working microvalve when (a) it is closed and (b) opened.

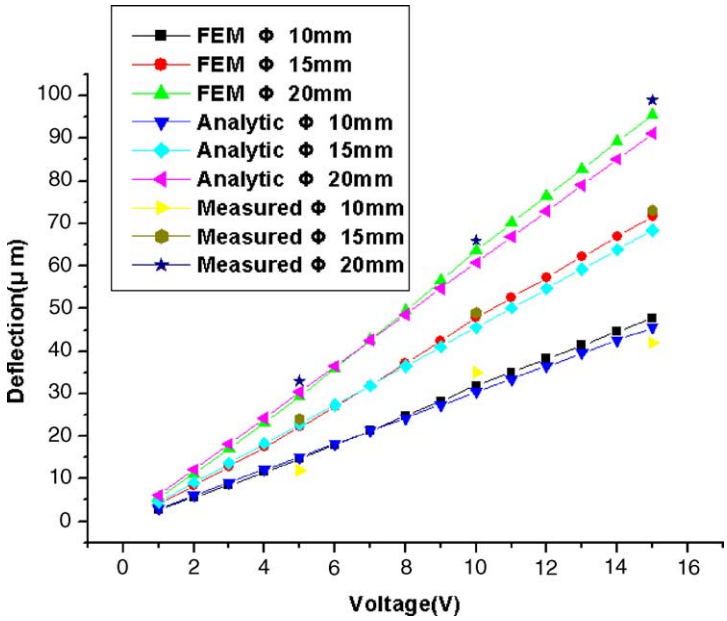

Fig. 4. Tip deflections of the microvalve as a function of applied voltages.

used for the simulation are listed in Table 2. The 3D model of the $\Phi = 10$ mm-type micro cantilever under applied voltage of 5 V was simulated, as shown in Fig. 5(a); the simulation results are shown in Fig. 5(b). At 5 V, the tip deflections for $\Phi = 10$, 15, and 20 mm-type micro cantilever were predicted as 15.2, 22.8, and 30.4 μm, respectively. The result is included in Fig. 4.

2.3. Fluidic analysis

When the microvalve is closed, gas is forced through the gaps between the microcantilevers and supporting structures. To evaluate this leakage rate, the Bernoulli and continuity equations for incompressible steady frictionless flow were solved [17]. The Bernoulli equation for the microvalve is

$$P_1 + \frac{1}{2}\rho {V_1}^2 = P_2 + \frac{1}{2}\rho {V_2}^2 \tag{3}$$

and the continuity equation is

$$Q = A_1 V_1 = A_2 V_2 \tag{4}$$

where ρ is the density of the fluid, Q the flow rate of leakage, V_1 the velocity of the flow before the microvalve, A_1 the

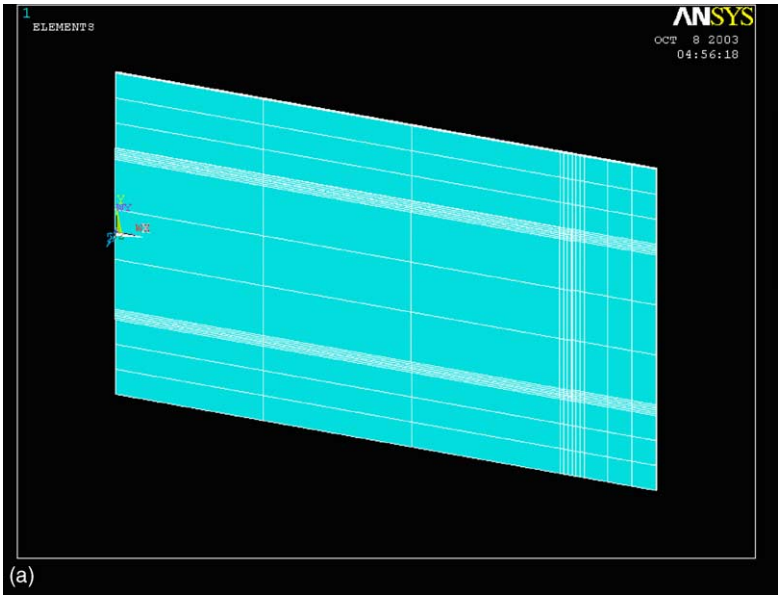

Fig. 5. (a) Simulation model of the micro cantilever and (b) simulation results.

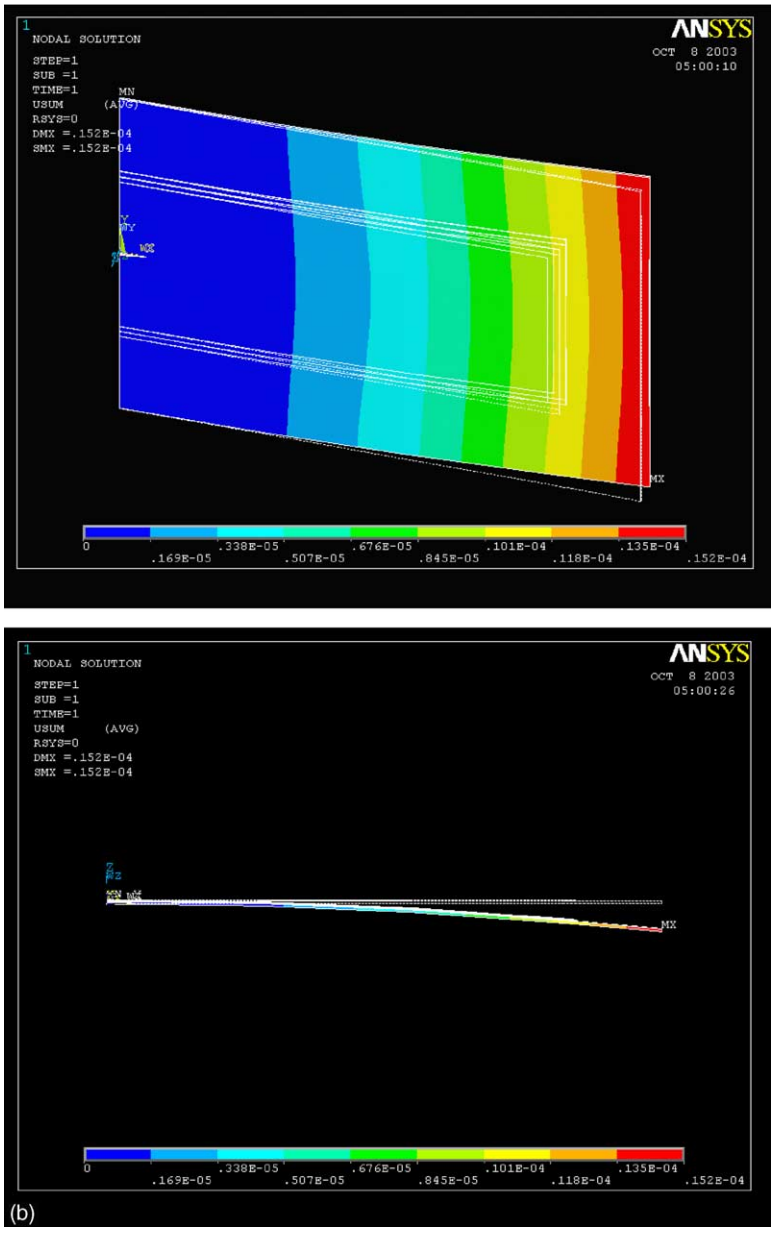

Fig. 5. (*Continued*).

Table 2
Dimensions of the micro cantilever

Thickness (μm)	Top Pt	0.15
	PZT	0.50
	Bottom Pt	0.15
	Ta	0.03
	Oxide	0.20
	Poly-Si	2.00
Lenth (μm)		450.00
Width (μm)		300.00

area of flow before the microvalve, V_2 the velocity after the microvalve, and A_2 is the area of gaps, which are illustrated in Fig. 6 (a). A_1 and A_2 can be expressed as follows:

$$A_1 = (2L + w)(b + 2w) \tag{5}$$

and

$$A_2 = 2w(2L + w) + bw \tag{6}$$

where L is the length of the cantilever, w the width of the gap and b is the width of the cantilever, which are also illustrated in Fig. 6(a). By combining Eqs. (3) and (4), the flow rate

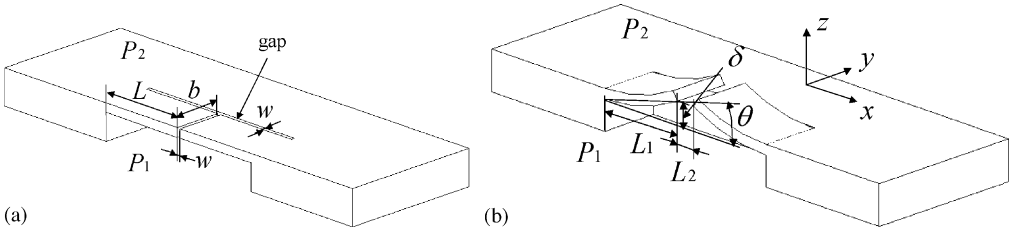

Fig. 6. Parameters of the microvalve model when (a) it is closed and (b) opened.

through the microvalve can be obtained as follows:

$$Q = A_1 \left[\frac{2(P_1 - P_2)}{\rho \left\{ \left(\frac{A_1}{A_2} \right)^2 - 1 \right\}} \right]^{1/2} \tag{7}$$

The calculated leakage rate for the $\Phi = 10$ mm-type micro cantilever was 20.4 μl/s with a pressure difference of 1000 Pa. The fluid was air, which density of 1.20 kg/m^3 at 20 °C, 1 atm. The results for the case of 0 V applied are shown in Fig. 7.

In the same way, the gas flow in the opened position was evaluated based on the Bernoulli and continuity equations. Gas flow was assumed in the y and z directions after passing the valves at the same condition that was applied to the leakage flow evaluation. The slope at the end of the cantilever applied with voltage is given by

$$\theta = \sin^{-1}\left(\frac{\delta}{L}\right) \tag{8}$$

where θ denotes the angle at the end of the cantilever measured from the x axis. Using Eq. (8), the x coordinate of the deflected tip L_1 can be written as

$$L_1 = L \cos\theta \tag{9}$$

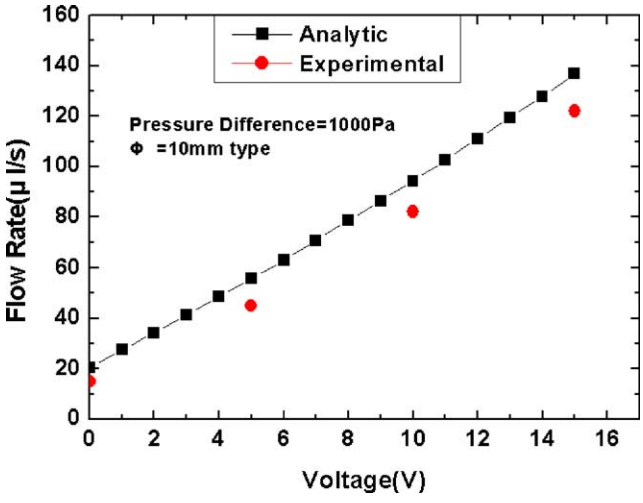

Fig. 7. Calculated and measured flow rates under given pressure difference.

Using Eq. (9), the distance L_2 between two ends of each deflected cantilevers can be calculated as

$$L_2 = 2(L - L_1) \tag{10}$$

This is illustrated in Fig. 6(b). Then the opened area A_2' due to the tip deflection can be calculated as

$$A_2' = 2L_1\delta + 2L_1 + bL_2 \tag{11}$$

Using Eqs. (7) and (11), the flow rate Q' through the microvalve can be determined as

$$Q' = A_1 \left[\frac{2(P_1 - P_2)}{\rho \left\{ \left(\frac{A_1}{A_2'} \right)^2 - 1 \right\}} \right]^{1/2} \tag{12}$$

For $\Phi = 10$ mm-type micro cantilever, the air flow rate of 136.8 μl/s was predicted at the pressure difference of 1000 Pa, 15 V applied. The properties of air were the same as those used in the leakage calculation. The results are also shown in Fig. 7.

2.4. Application

The microvalve that we have developed is not only slim to suit miniaturization, but also effective in controlling a refrigerant. Conventional micro compressors using motors or PZT actuators are difficult to miniaturize. So, the most promising micro compressor structure is the membrane type with microvalves that can pump and compress working fluid in active micro cooling systems to enhance the performance of electronic chips. Fig. 8 shows the conceptual design of a micro cooler. The system size is $\Phi = 10 \times 5$ mm, incorporating the microvalves on membranes, and is composed of a condenser, an insulation layer, a compressor with an expansion nozzle, another insulation layer, and an evaporator. It can be directly installed on a CPU or electronic chips and can accept a large amount of heat (up to 60 W) from the evaporator and reject it at the condenser. The micro cooler will work with a refrigerating cycle.

An important part of the micro cooler is the micro compressor layer. The conceptual design of the micro compressor is shown in Fig. 9(a). It has multiple sub-units that can compress the working fluid. The sub-units are symmetrical with double membranes actuated by PZT films and double flap valves with PZT films. The membranes can vibrate vertically

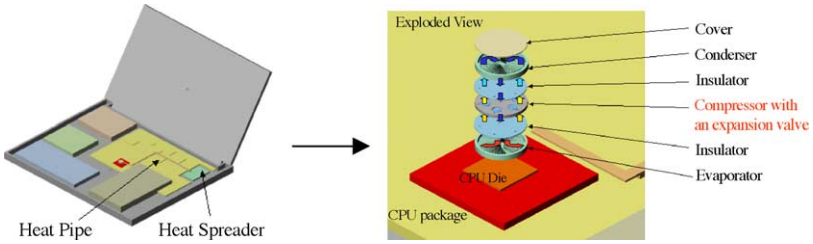

Fig. 8. Conceptual design of a micro cooler.

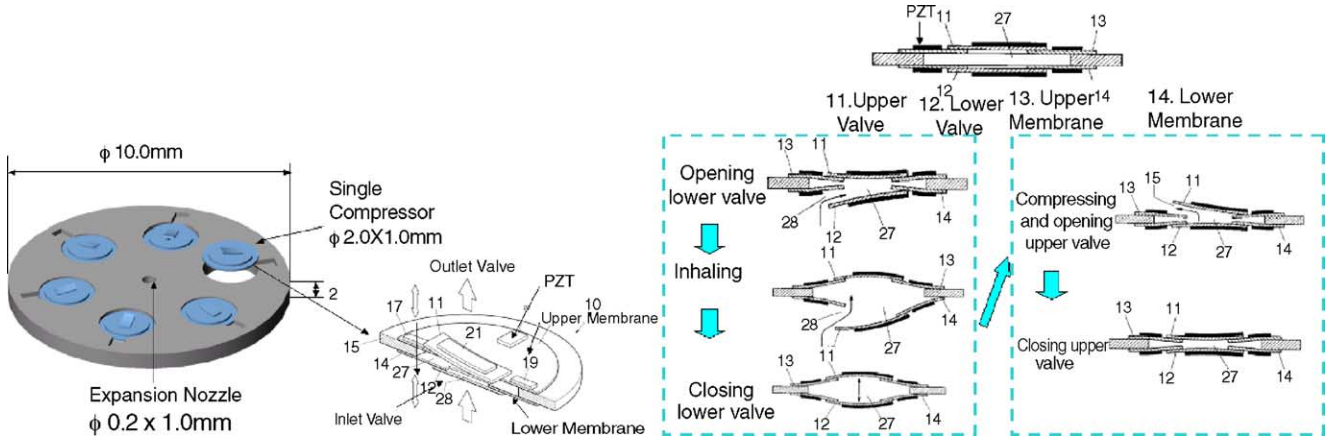

Fig. 9. (a) The conceptual design of the micro compressor and (b) working principle.

to change the chamber volume and the flap valves control the flow of the working fluid. It goes through five steps to compress the fluid as shown in Fig. 9(b). First, the lower flap valve is opened to prepare the sequence; second, the double membranes will inflate to inhale the fluid into the chamber; third, the lower valve is closed to compress the chamber volume and raise the pressure in an adiabatic environment because this layer will be placed between isolation layers; and lastly, the upper valve is opened to allow the compressed fluid to escape from the evaporator to the condenser with the heat generated from the chip. And then, the upper valve is closed to repeat the cycle.

In the first stage of this project, we developed the slim type microvalve driven by PZT films. The design features and the performance result will be used to further develop microvalves in the micro cooler.

3. Fabrication

3.1. Micro fabrication

Fig. 10 shows the eight main processes for fabricating the microvalve: deposition of oxide/Ta/Pt/PZT/Pt layers on a silicon on insulator (SOI) wafer (steps 1–3), etching the oxide/poly-Si/oxide/Ta/Pt/PZT/Pt layers from the top (steps 4–5), lift off process (step 6) and etching oxide/Si from the backside (steps 7–8).

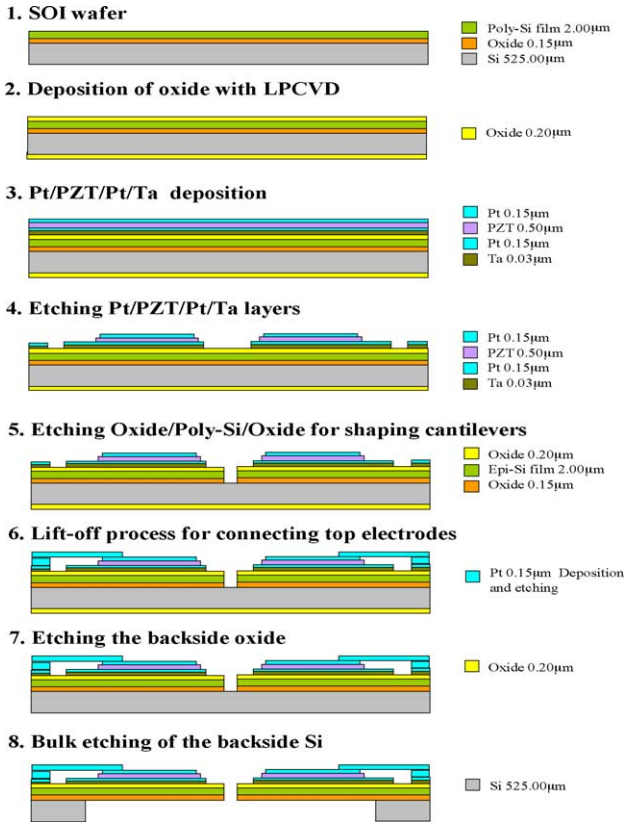

Fig. 10. Fabrication process of the microvalve.

We started the fabrication of the microvalve with a 4 in. SOI wafer. The carrier wafer (1 0 0) was 525 μm-thick; a buried SiO_2 layer was 0.15 μm-thick; and the device layer was 2 μm-thick. A 0.2 μm-thick oxide was thermally grown on both sides of the wafer. Then, 0.15 μm-thick tantalum (Ta) layer was deposited to adhere the nitride layer to the platinum (Pt) layer. Subsequently, 0.5 μm-thick PZT ($PbZr_{0.52}Ti_{0.48}O_3$) layer was prepared with chemical solution deposition (CSD) (which will be explained in next paragraph in detail). Afterwards, the top Pt electrode was sputtered to a thickness of 0.15 μm. To prevent short circuits between the top electrodes and the bottom electrodes, the top electrodes were structured into smaller rectangles than those of the PZT pattern by reactive ion etching (RIE) process. The etching rate was 0.16 μm/min with a Cl_2 plasma at an applied bias of 300 V and chamber pressure of 8 μbar. The PZT films were patterned by RIE process with a photoresist mask. The 0.5 μm-thick PZT was etched by Cl_2/BCl_3 plasma at an applied bias of 300 V and chamber pressure of 8 μbar. The etch rate was 0.2 μm/min. The PZT film was etched slightly more than the PZT film thickness, so the bottom electrode appeared under the PZT after etching. Then the bottom Pt layer was patterned by the parameters used for the top electrode. After each etching step, the remaining photoresist was removed with O_2 plasma at flow rate of 200 sccm at 300 W for 10 min.

To shape the cantilevers with 4 μm gaps, SiO_2 layer was patterned by magnetically enhanced reactive ion etching (MERIE) with photoresist mask. CF_4, CHF_3, and Ar were supplied at rates of 25, 5, and 70 sccm, respectively, at an applied r.f. power of 600 W, a chamber pressure of 173 μbar, and a magnetic field of 60 G. The SiO_2 layer was etched at a rate of 0.34 μm/min. After this step, the poly-Si layer was etched by inductively coupled plasma (ICP) with a photoresist mask of the same patterns. Cl_2, He, and O_2 gas were supplied at rates of 100, 8 and 10 sccm, respectively. The measured etch rate was 0.45 μm/min, with the applied r.f. power of 300 W and chamber pressure of 2.7 μbar. Then the buried SiO_2 layer was also structured by MERIE with the same mask patterns of the photoresist. CF_4, CHF_3, and Ar were supplied at rates of 25, 5, and 70 sccm, respectively, at an applied r.f. power of 600 W, a chamber pressure of 173 μbar, and a magnetic field of 60 G, which were same the etching process condition of the upper SiO_2 layer. And the SiO_2 layer was etched at a rate of 0.33 μm/min.

For the lift-off process, additional Pt layer was sputtered with a thickness of 0.15 μm on coated photoresist layer that had contact hole patterns. Before this step, photoresist must be developed so that the top electrodes come into good contact with the additional Pt layer for the lift-off. The Pt layer was etched by reactive ion etching process at the same conditions used for etching the top electrodes. After this Pt layer was etched, the remaining photoresist was removed with O_2 plasma of 300 W for 10 min, at a rate of 200 sccm.

The remaining backside SiO_2 layer was etched at the same condition as step 5. Finally, bulk Si was etched from the backside by ICP with C_4F_8, SF_6 and Ar gas plasma. In this process, a clean chamber was required since residual materials from other users were deposited on the sidewalls of the patterns. So the chamber was cleaned before etching. Main etching was done carefully so that the SiO_2 layer can stop the etching process and the front patterns were protected with photoresist and a bare Si wafer. First, the 500 μm-thick bulk Si was etched from the backside by C_4F_8, SF_6, and Ar at rates of 0.5, 100, and 30 sccm, respectively, at an applied r.f. power of 825 W and chamber pressure of 31 μbar. The measured etch rate was 2.7 μm/min. Then, the remaining 25 μm Si layer was etched with the same conditions that were used for the 500 μm Si etch process. Photoresist was used as an etching mask, and SiO_2 layer stopped the etching process successfully. Cantilevers were released after the bare Si wafer was separated chemically from the main wafer. Each sample was separated from the whole wafer not by dicing but by patterning the cutting lines that were originally included in the photoresist mask patterns to achieve the bulk Si etching process. Samples were fabricated well.

3.2. PZT film deposition

Previous coating techniques were investigated for the PZT film deposition. PZT films can be deposited by physical techniques such as ion beam sputtering, r.f. planar magnetron sputtering and dc magnetron sputtering [18]. Recently, PZT films have been synthesized by several chemical methods such as sol–gel method, metal organic chemical vapour deposition (MOCVD), dip-coating, and screen-press. Among them, the sol–gel deposition is widely used because it is compatible to photolithography, can be processed at low temperatures, can coat large areas, and can control composition precisely. We prepared the PZT film between two Pt electrodes by chemical solution deposition. Sol–gel precursor of Pb:Zr:Ti = 110:52:48 was used. The PZT thin-film with this composition has been widely used because of its good piezoelectric and ferroelectric properties. The PZT film was prepared by spin-coating the solution on the Pt and SiO_2 layer deposited SIMOX wafer at 4000 rpm for 20 s. To remove the solvent, the film was baked on a hot plate at 300 °C for 5 min and 450 °C for 5 min in the furnace. Then, the film was thermally annealed rapidly (RTA) at 650 °C for 2 min to crystallize the amorphous film. A PZT film of 0.5 μm thickness with smooth and crack-free surface was obtained.

4. Microvalve operation

4.1. PZT film properties

We evaluated the ferroelectric property of the deposited PZT film with Precision Pro (Radiant Technologies Inc.), and the polarization-applied voltage hysteresis loop is shown in Fig. 11(a). This property was measured on the substrate of Pt/Ta/oxide/SIMOX with an upper electrode of an array

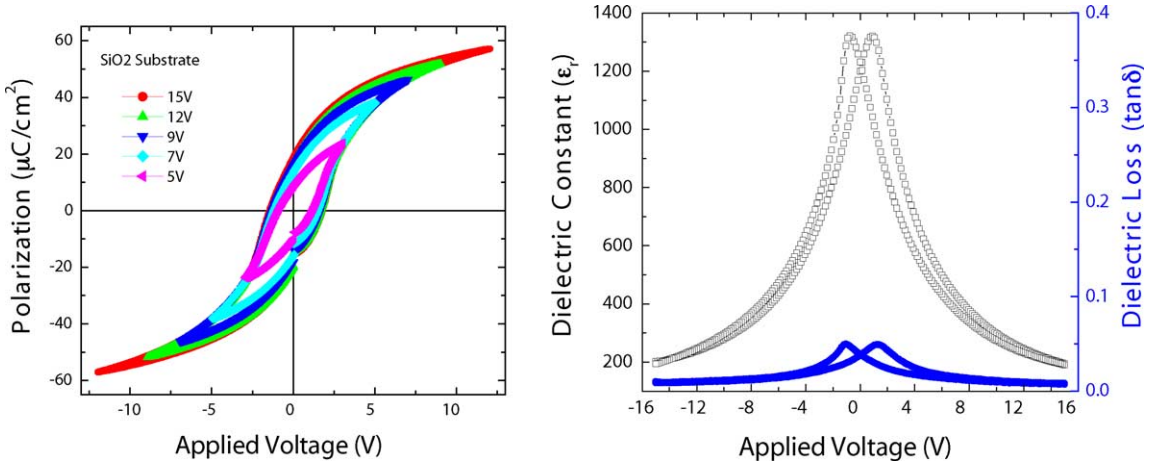

Fig. 11. (a) *P–V* hysteresis loop of PZT film, and (b) dielectric constant and dielectric loss of the PZT film on SiO_2 substrate.

of sputtered Pt. Good ferroelectric property of the deposited PZT film was confirmed.

Fig. 11(b) shows the variation of dielectric constant and dielectric loss with applied voltages, which was measured with impedance analyzer 4294 (Agilent). The dielectric constant decreased from 1300 to 200 as the applied voltage changed from 2 to 15 V. The dielectric loss was less than 0.05 and decreased from 0.05 to 0.01 as the voltage changed from 2 to 15 V.

X-ray diffractometer (XRD) analysis was carried out to investigate the crystalline structure and orientation of the films. XRD patterns of the PZT films are shown in Fig. 12. This figure shows that the perovskite phase of PZT films in the polycrystalline state had strong (1 1 1) orientations on (1 1 1) Pt layer.

4.2. Microvalve operation

We measured the piezoelectric actuation using the laser interferometer, which can measure the tip deflection of the fabricated microvalve. Tip deflection was observed when sine wave signal was applied at the bipolar voltage of ±15 V and frequency of 2 Hz. And the tip displacement as a function of applied voltage was measured; the displacement was proportional to the input voltage. The measured tip displacement of the $\Phi = 10$ mm-type cantilever was 12 μm at 5 V, which agrees well to the estimated values of 15.2 μm obtained from FEM analysis and 14.8 μm from the evaluation.

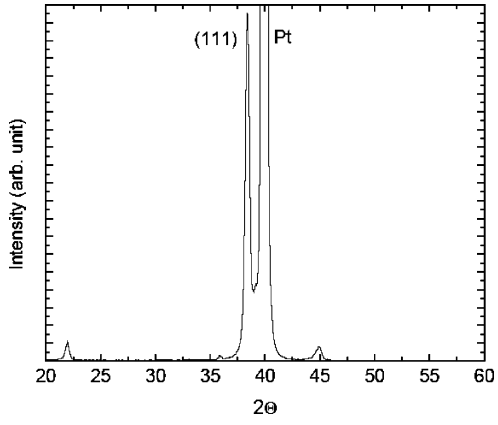

Fig. 12. X-ray diffraction patterns of PZT films.

The leakage rate of air of the $\Phi = 10$ mm-type microvalve in closed position was measured and was found to be 15 μl/s with the pressure difference of 1000 Pa. The maximum flow rate of 122 μl/s was obtained with the same pressure difference and applied voltage of 15 V. This agrees well with the predicted value, which was compared with the measured value, as shown in Fig. 7. The opening and closing time was measured to be 500 ms, which was smaller than the required time of 1 s. The maximum thickness of the fabricated microvalve was 527 μm, which was thinner than the desired value of 600 μm.

5. Discussion

In designing the microcantilevers, we utilized the Young's modulus data of the PZT bulk and the piezoelectric coefficient e_{31} of perovskite phase of PZT films with (1 1 1) orientations on (1 1 1) Pt layer. The experimental results of the tip deflections fit well with the prediction, so these values were considered to be useful. The target deflection was designed to be 45 μm and the tip deflection of 42 μm was obtained at 15 V.

The microvalves worked well with a maximum flow rate of 122 μl/s, which is somewhat lower than the expected value, at 1000 Pa pressure difference. This result was obtained because frictionless flow was assumed. The leakage rate was relatively large compared to that of the previous work because the limitation of the photolithography process. Due to the 1 μm wave length of ultraviolet (UV) light that was exposed to the photoresist, the minimum reliable resolution of gap patterns was 4 μm. A micro flap valve

structure that can cover these gaps will be studied in future work.

6. Conclusions

The slim type microvalves for micro fluidic systems were designed and fabricated. Small gaps between the supporting structures can reduce reverse leakage of the working fluid, and large 120 cantilevers (450 μm × 300 μm of the $\Phi = 10$ mm-type) can produce more displacement. We measured the tip deflection at different voltages from 1 V to 15 V. The measured tip displacement of the $\Phi = 10$ mm-type was 12 μm at 5 V, and this value agreed well to the estimated values of 15.2 μm obtained from FEM analysis and 14.8 μm from the evaluation. The fabricated microvalve worked with the flow rate of 122 μl/s at 1000 Pa pressure difference of air at 15 V.

Due to the slim structure, it can be easily incorporated into other microfluidic devices. Further development will concentrate on reducing the leakages and integrating the microvalve into micro fluidic system such as the micro cooler.

Acknowledgement

This research was supported by Micro Thermal System Research Center at Seoul National University.

References

[1] P. Selvaganapathy, E.T. Carlen, C.H. Mastrangelo, Electrothermally actuated inline microfluidic valve, Sens. Actuators A 104 (2003) 275–282.
[2] D.C. Roberts, H. Li, J.L. Steyn, O. Yaglioglu, S.M. Spearing, M.A. Schmidt, N.W. Hagood, A piezoelectric microvalve for compact high-frequency, high-differential pressure hydraulic micropumping systems, J. Microelectromech. Syst. 12 (2003) 81–92.
[3] M. Capanu, J.G. Boyd, P.J. Hesketh, Design, fabrication, and testing of a bistable electromagnetically actuated microvalve, J. Microelectromech. Syst. 9 (2000) 181–189.
[4] H. Jerman, Electrically-activated, normally-closed diaphragm valves-dkjdot, in: Tech. Digest, Transducers: The International Conference on Solid-State Sensors and Actuators, San Francisco, CA, USA, June 24–27, 1991, pp. 1045–1048.
[5] C.M. Pemble, B.C. Towe, A miniature shape memory alloy pinch valve, Sens. Actuators A 77 (1999) 145–148.
[6] T. Itoh, C. Lee, G. Sasaki, T. Suga, Sol-gel derived PZT force sensor for scanning force microscopy, Mater. Chem. Phys. 44 (1996) 25–29.
[7] S.S. Lee, R.M. White, Piezoelectric cantilever voltage-to-frequency converter, Sens. Actuators A 71 (1998) 153–157.
[8] K. Yamashita, H. Katata, M. Okuyama, H. Miyoshi, G. Kato, S. Aoyagi, Y. Suzuki, Arrayed ultrasonic microsensors with high directivity for in-air use using PZT thin film on silicon diaphragms, Sens. Actuators A 97–98 (2002) 302–307.
[9] M. Koch, N. Harris, A.G.R. Evans, N.M. White, A. Brunnschweiler, A novel micromachined pump based on thick-film piezoelectric actuation, Sens. Actuators A 70 (1998) 98–103.
[10] A.M. Flynn, L.S. Tavrow, S.F. Bart, R.A. Brooks, D.J. Ehrlich, K.R. Udayakumar, L.E. Cross, Piezoelectric micromotors for microrobots, J. Microelectromech. Syst. 1 (1992) 44–51.
[11] H. Kueppers, T. Leuerer, U. Schnakenberg, W. Mokwa, M. Hoffmann, T. Schneller, U. Boettger, R. Waser, PZT thin films for piezoelectric microactuator applications, Sens. Actuators A 97–98 (2002) 680–684.
[12] S.J. Gross, S. Tadigadapa, T.N. Jackson, S. Trolier-McKinstry, Q.Q. Zhang, Lead-zirconate-titanate-based piezoelectric micromachined switch, Appl. Phys. Lett. 83 (2003) 174–176.
[13] J.G. Smits, W. Choi, The constituent equations of piezoelectric heterogeneous bimorphs, IEEE Trans. Ultrason. Ferroelectr. Freq. Control 38 (1991) 256–270.
[14] W.H. Ryu, Y.-C. Chung, D.-K. Choi, C.S. Yoon, C.K. Kim, Y.-H. Kim, Computer simulation of the resonance characteristics and the sensitivity of cantilever-shaped Al/PZT/RuO_2 biosensor, Sens. Actuators B 97 (2004) 98–102.
[15] M. Gad-El-Hak, The MEMS Handbook, CRC Press, 2001.
[16] I. Kanno, H. Kotera, K. Wasa, Measurement of transverse piezoelectric properties of PZT thin films, Sens. Actuators A 107 (2003) 68–74.
[17] F. M. White, Fluid Mechanics, McGraw-Hill, 1994.
[18] L. Du, G. Kwon, F. Arai, T. Fukuda, K. Itoigawa, Y. Tukahara, Structure design of micro touch sensor array, Sens. Actuators A 107 (2003) 7–13.

Biographies

Hyonse Kim received BS degree in mechanical design and production engineering from Seoul National University, Seoul, Korea, in 1998 and MS degree in mechanical and aerospace engineering from Seoul National University in 2000. He is currently a PhD candidate in Seoul National University. His research topics include micro electro mechanical systems (MEMS) driven by PZT films and micro cooler for electronic chips.

Gil Ho Yoon received BS degree in mechanical design and production engineering from Seoul National University in 1998 and MS degree in mechanical and aerospace engineering from Seoul National University in 2000. He received PhD degree in mechanical and aerospace engineering from Seoul National University in 2004.

Chihyun In received BS degree in mechanical design and production engineering from Seoul National University in 1998 and MS degree in mechanical and aerospace engineering from Seoul National University in 2000. He is now working in MEMS division, DAEWOO Electronics Corp. in Seoul, Korea.

Jongwon Kim received BS degree in mechanical engineering from Seoul National University in 1978 and MS degree in mechanical and aerospace engineering from KAIST (Korea Institute of Science and Technology), Daejeon, Korea, in 1980. He received PhD degree in mechanical engineering from University of Wisconsin-Madison, USA, in 1987. He worked with Daewoo Heavy Industry & Machinery, Changwon, Korea, from 1980 to 1984. From 1987 to 1989, he was Director of Central R&D Division at Daewoo Heavy Industry & Machinery. From 1989 to 1993, he was researcher at the Automation and Systems Research Institute at Seoul National University. In August 1993, he became professor of mechanical and aerospace engineering at Seoul National University. His research topics include robust design of micro and macro mechanical systems.